2018

Improving Measurement Sensitivity for a Displacement Sensor based on Self-Mixing Effect

Yuxi Ruan
University of Wollongong, yr776@uowmail.edu.au

Bin Liu
University of Wollongong, bl987@uowmail.edu.au

Yanguang Yu
University of Wollongong, yanguang@uow.edu.au

Jiangtao Xi
University of Wollongong, jiangtao@uow.edu.au

Qinghua Guo
University of Wollongong, qguo@uow.edu.au

See next page for additional authors

Improving Measurement Sensitivity for a Displacement Sensor based on Self-Mixing Effect

Abstract

When a part of light emitted by a laser is back-reflected or back-scattered from an external target and re-enters the laser cavity, both the laser intensity and its wavelength can be modulated. This is so called Self-Mixing Effect (SME). An SME based displacement sensor is featured with compact physical setup and interferometric measurement resolution. However, when a target has a surface with very low reflectivity, the sensing signal is very weak and noisy. The system may even lose its sensing capability. It is desired to develop a method for improving the sensing performance in this case. We propose a configuration of dual external cavities for the SME based sensing system, where one of the cavities is used to provide pre-feedback for improving the sensing sensitivity and the other is related to the target to be measured. Firstly, a sensing model is derived for the proposed configuration and shows that the magnitude of the sensing signal can be enhanced by setting the pre-feedback cavity with suitable location and high optical feedback strength. Then experimental investigations are conducted to demonstrate the feasibility of the proposed approach. This paper provides an important guidance for designing an SME based sensor with high sensitivity.

Disciplines

Engineering | Science and Technology Studies

Publication Details

Y. Ruan, B. Liu, Y. Yu, J. Xi, Q. Guo & J. Tong, "Improving Measurement Sensitivity for a Displacement Sensor based on Self-Mixing Effect," IEEE Photonics Journal, vol. 10, (6) pp. 6804010-1-6804010-11, 2018.

Authors

Yuxi Ruan, Bin Liu, Yanguang Yu, Jiangtao Xi, Qinghua Guo, and Jun Tong

IEEE Photonics Journal
An IEEE Photonics Society Publication

Improving Measurement Sensitivity for a Displacement Sensor Based on Self-Mixing Effect

Volume 10, Number 6, December 2018

Yuxi Ruan
Bin Liu
Yanguang Yu
Jiangtao Xi
Qinghua Guo
Jun Tong

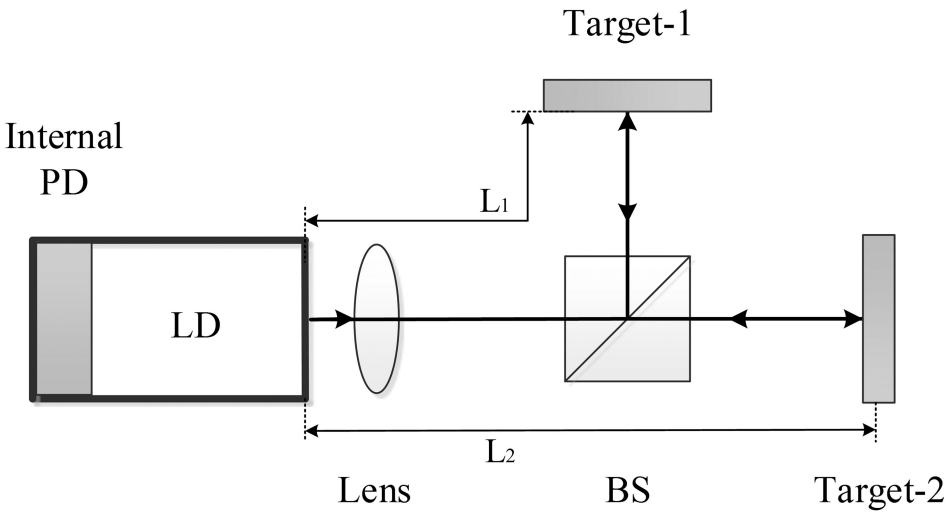

Self-Mixing Interferometry with pre-feedback to achieve high sensing sensitivity

DOI: 10.1109/JPHOT.2018.2876117
1943-0655 © 2018 IEEE

Improving Measurement Sensitivity for a Displacement Sensor Based on Self-Mixing Effect

Yuxi Ruan, Bin Liu, Yanguang Yu, Jiangtao Xi, Qinghua Guo, and Jun Tong

University of Wollongong, Northfields Avenue, Wollongong, NSW 2522, Australia

DOI:10.1109/JPHOT.2018.2876117

Manuscript received September 3, 2018; revised October 9, 2018; accepted October 11, 2018. Date of publication October 15, 2018; date of current version October 29, 2018. Corresponding author: Yanguang Yu (e-mail yanguang@uow.edu.au).

Abstract: When a part of light emitted by a laser is back-reflected or back-scattered from an external target and re-enters the laser cavity, both the laser intensity and its wavelength can be modulated. This is so-called self-mixing effect (SME). An SME-based displacement sensor is featured with compact physical setup and interferometric measurement resolution. However, when a target has a surface with very low reflectivity, the sensing signal is very weak and noisy. The system may even lose its sensing capability. It is desired to develop a method for improving the sensing performance in this case. We propose a configuration of dual external cavities for the SME-based sensing system, where one of the cavities is used to provide prefeedback for improving the sensing sensitivity and the other is related to the target to be measured. First, a sensing model is derived for the proposed configuration and shows that the magnitude of the sensing signal can be enhanced by setting the prefeedback cavity with suitable location and high optical feedback strength. Then, experimental investigations are conducted to demonstrate the feasibility of the proposed approach. This paper provides an important guidance for designing an SME-based sensor with high sensitivity.

Index Terms: Displacement sensor, laser sensing, measurement sensitivity, optical feedback interferometry, self-mixing interferometry.

1. Introduction

As a promising non-contact sensing technology, Self-Mixing Interferometry (SMI) has attracted much attention of researchers in recent decades. The SMI is based on the Self-Mixing Effect (SME) that occurs when a fraction of light back-reflected or back-scattered by an external target re-enters the laser inside cavity [1]–[3]. In this case, both the laser output power and frequency are modulated. The modulated laser power carries the information related to the movement of the external target as well as the parameters of the laser. Hence SME based sensing can be developed for various applications. A typical SMI system consists of a laser diode (LD), a photodiode (PD) packaged in the rear of the LD, a focusing lens and an external target to be measured, as shown in Fig. 1. As a minimum part-count scheme, various SMI-based measurements and detections have been reported such as measurement of displacement, velocity, vibration, laser related parameters, thickness, mechanical resonance [4]–[13], etc. Recent years, the SME based sensing has been extended for imaging, material parameters measurement, near-field microscopy, chaotic radar, acoustic detection, biomedical applications [11], [14]–[16], etc.

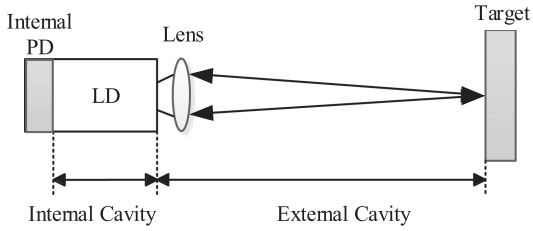

Fig. 1. Basic structure of an SMI system.

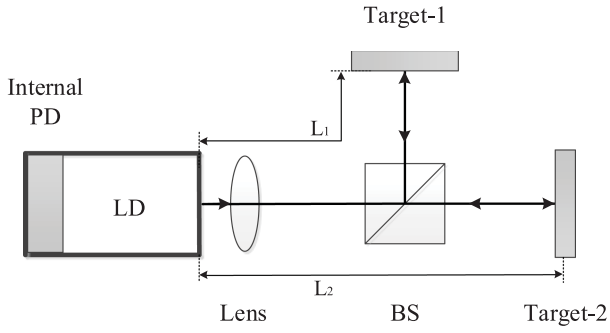

Fig. 2. Modified SMI structure with a pre-feedback.

An SME sensing system for displacement measurement has a resolution same as the traditional Michelson interferometer [1]. For a sensing signal generated by an SMI system (called SMI signal in below), one fringe variation in the SMI signal corresponds to the target displacement of half laser wavelength. The magnitude of the SMI signal depends on the system's feedback strength and the parameters of the LD.

In some practical cases, a target surface has very low reflectivity and thus is unable to provide adequate feedback light into the LD. In this condition, the observed SMI signal is very weak and blurred. The sensing sensitivity of the system is degraded and the SMI signal may even lost its sensing ability. To solve this problem, generally, a mirror or a piece of material with high reflectivity can be glued on the target to provide a high enough feedback light and gain an SMI signal with intensified magnitude. However, in some applications, such as in biomedical field or with a fluid surface, it is not possible to add any material on the measured target. Therefore, it is strongly desired to develop a method to improve the SMI system to enhance its sensing sensitivity.

In this work, we propose to apply a pre-feedback to an SMI displacement sensor so that its sensing sensitivity can be considerably improved. Staring from the well-known Lang and Kobayashi equations, a theoretical model is derived for a modified SMI sensing model with a pre-feedback. By comparison of the SMI sensing system with and without the pre-feedback, we found the location of the pre-feedback target and its feedback strength have significant influence on the magnitude of the SMI signal. An experimental set-up is built for the investigation on how to enhance the sensitivity for an SME based displacement sensor.

2. Theory

A general SMI system can be modified by adding a pre-feedback shown as Fig. 2. It can be seen that the LD has two external targets. Target-1 is the measured target with a very low reflectivity on its surface. Target-2 is used to provide a pre-feedback.

It is well known that the dynamics of a laser diode with optical feedback can be described by the Lang and Kobayashi (L-K) equations [17]. With the system shown in Fig. 2, we can modify the L-K

TABLE 1
Physical Meanings and Values of the Parameters in LK Equations

Symbol	Physical Meaning	Value
G_N	Modal gain coefficient	$8.1\times10^{-13}\,m^3s^{-1}$
N_0	Carrier density at transparency	$1.1\times10^{24}\,m^{-3}$
ε	Nonlinear gain compression coefficient	$2.5\times10^{-23}\,m^3$
Γ	Confinement factor	0
τ_p	Photon life time	$2.0\times10^{-12}\,s$
τ_{in}	Internal cavity round-trip time	$8.0\times10^{-12}\,s$
τ_s	Carrier life time	$2.0\times10^{-9}\,s$
κ	Feedback strength	
τ	External cavity round trip time, $\tau = 2L/c$, where L is external cavity length, c is speed of light	
ω_0	Angular frequency of solitary laser $\omega_0 = 2\pi c/\lambda_0$, where λ_0 is the laser wavelength	
α	Line-width enhancement factor	3.0
J	Injection current density	

equations as below,

$$\frac{dE(t)}{dt} = \frac{1}{2}\left\{G\left[N(t), E(t)\right] - \frac{1}{\tau_p}\right\}E(t) + \frac{\kappa_1}{\tau_{in}}\cdot E(t-\tau_1)\cdot\cos\left[\omega_0\tau_1 + \phi(t) - \phi(t-\tau_1)\right] + \frac{\kappa_2}{\tau_{in}}\cdot E(t-\tau_2)\cdot\cos\left[\omega_0\tau_2 + \phi(t) - \phi(t-\tau_2)\right] \quad (1)$$

$$\frac{d\phi(t)}{dt} = \frac{1}{2}\alpha\left\{G\left[N(t), E(t)\right] - \frac{1}{\tau_p}\right\} - \frac{\kappa_1}{\tau_{in}}\cdot\frac{E(t-\tau_1)}{E(t)}\cdot\sin\left[\omega_0\tau_1 + \phi(t) - \phi(t-\tau_1)\right] - \frac{\kappa_2}{\tau_{in}}\cdot\frac{E(t-\tau_2)}{E(t)}\cdot\sin\left[\omega_0\tau_2 + \phi(t) - \phi(t-\tau_2)\right] \quad (2)$$

$$\frac{dN(t)}{dt} = J - \frac{N(t)}{\tau_s} - G\left[N(t), E(t)\right]E^2(t) \quad (3)$$

In Eq.(1)–Eq.(3), there are three variables named as electric field amplitude $E(t)$, electric field phase $\phi(t)$ and carrier density $N(t)$. $\phi(t)$ is given by $\phi(t) = [\omega(t) - \omega_0]\,t$, where $\omega(t)$ is the instantaneous optical angular frequency for an LD with optical feedback, ω_0 is the unperturbed optical angular frequency for a solitary LD. $G[N(t), E(t)] = G_N[N(t) - N_0][1 - \varepsilon\Gamma E^2(t)]$ is the modal gain per unit time, and the nonlinear gain is ignored in this work. Therefore, $G[N(t), E(t)] = G_N(N_s - N_0)$. The physical meanings of the symbols appearing in Eq.(1)–Eq.(3) and the values of the parameters are shown in Table 1.

The SMI sensing model can be derived by solving the L-K equations Eq.(1)–Eq.(3) to obtain the steady solutions for $E(t)$, $N(t)$ and $\omega(t)$, denoted as E_s, N_s and ω_s respectively, by setting $dE(t)/dt = 0$, $d\phi(t)/dt = \omega_s - \omega_0$ and $dN(t)/dt = 0$.

To express the variation of the laser intensity $E(t)^2$ induced by the two targets, we need to find the steady solutions of Eq.(1)–Eq.(3). By setting $d\phi(t)/dt = \omega_s - \omega_0$, we get,

$$\omega_0\tau_1 = \omega_s\tau_1 + \frac{\kappa_1}{\tau_{in}}\tau_1\sqrt{1+\alpha^2}\sin\left(\omega_s\tau_1 + \arctan(\alpha)\right) + \frac{\kappa_2}{\tau_{in}}\tau_1\sqrt{1+\alpha^2}\sin\left(\omega_s\tau_2 + \arctan(\alpha)\right) \quad (4)$$

By setting $dE(t)/dt = 0$, we get,

$$N_s = N_0 + \frac{1}{G_N \tau_p} - \frac{2\kappa_1 \cos(\omega_s \tau_1)}{\tau_{in} G_N} - \frac{2\kappa_2 \cos(\omega_s \tau_2)}{\tau_{in} G_N} \tag{5}$$

By setting $dN(t)/dt = 0$, we get,

$$E_s{}^2 = \frac{J - N_s/\tau_s}{G_N(N_s - N_0)} \tag{6}$$

Substituting Eq.(5) into Eq.(6), we have,

$$E_s{}^2 = \frac{\frac{\tau_p}{\tau_s} * \left(J\tau_s - N_0 - \frac{1}{G_N \tau_p} + \frac{2\kappa_1 \cos(\omega_s \tau_1)}{\tau_{in} G_N} + \frac{2\kappa_2 \cos(\omega_s \tau_2)}{\tau_{in} G_N}\right)}{1 - \frac{2\tau_p \kappa_1 \cos(\omega_s \tau_1)}{\tau_{in}} - \frac{2\tau_p \kappa_2 \cos(\omega_s \tau_2)}{\tau_{in}}} \tag{7}$$

Eq.(4) and Eq.(7) are the proposed model for the SMI sensor with pre-feedback. It can be seen from Eq.(4) and Eq.(7) that if Target-2 related terms are removed Eq.(4) and Eq.(7) are reduced to

$$E^2_{s\_\text{Target}-1} = \frac{\frac{\tau_p}{\tau_s} * \left(J\tau_s - N_0 - \frac{1}{G_N \tau_p} + \frac{2\kappa_1 \cos(\omega_s \tau_1)}{\tau_{in} G_N}\right)}{1 - \frac{2\kappa_1 \tau_p \cos(\omega_s \tau_1)}{\tau_{in}}} \tag{8}$$

$$\omega_0 \tau_1 = \omega_s \tau_1 + \frac{\kappa_1}{\tau_{in}} \tau_1 \sqrt{1 + \alpha^2} \sin(\omega_s \tau_1 + \arctan(\alpha)) \tag{9}$$

Eq.(8) and Eq.(9) are SMI model with single target which were reported in many literatures [1]. With pre-feedback, Target-1 is moving and its surface has very low reflectivity and Target-2 is stationary and provides a high pre-feedback. Hence, we have $\kappa_2 \gg \kappa_1$. Since Target-1 has a very low reflectivity ($\kappa_1 \ll 0.01$) and thus $\frac{2\kappa_1 \tau_p \cos(\omega_s \tau_1)}{\tau_{in}} \ll 1$. For the convenience of comparison, we ignore $\frac{2\kappa_1 \tau_p \cos(\omega_s \tau_1)}{\tau_{in}}$ in the denominators of Eq.(7) and Eq.(8), then Eq.(7) and Eq.(8) can be approximated as the following two equations respectively,

$$E_s{}^2 = \frac{DC + \frac{\tau_p}{\tau_s} * \left(\frac{2\kappa_2 \cos(\omega_s \tau_2)}{\tau_{in} G_N} + \frac{2\kappa_1 \cos(\omega_s \tau_1)}{\tau_{in} G_N}\right)}{1 - \frac{2\tau_p \kappa_2 \cos(\omega_s \tau_2)}{\tau_{in}}} \tag{10}$$

$$E^2_{s\_\text{Target}-1} = DC + \frac{\tau_p}{\tau_s} * \frac{2\kappa_1 \cos(\omega_s \tau_1)}{\tau_{in} G_N} \tag{11}$$

Where $DC = \frac{\tau_p}{\tau_s} * (J\tau_s - N_0 - \frac{1}{G_N \tau_p})$. The DC value is determined by the LD ineternal parameters and the injection current. It can be treated as a constant once the physical system is established.

The displacement information (L_1) relevant to Target-1 movement is carried in the term of $\cos(\omega_s \tau_1)$ in Eq.(10) and Eq.(11) through $\tau_1 = 2L_1/c$. To describe the sensing of the displacements, we introduce ΔP_s and $\Delta P_{s\_\text{Target}-1}$ to represent the variation part in Eq.(10) and Eq.(11). Then we have,

$$\Delta P_s = E_s^2 - DC' = \frac{\frac{\tau_p}{\tau_s} * \frac{2\kappa_1 \cos(\omega_s \tau_1)}{\tau_{in} G_N}}{1 - \frac{2\tau_p \kappa_2 \cos(\omega_s \tau_2)}{\tau_{in}}} \tag{12}$$

$$\Delta P_{s\_\text{Target}-1} = E^2_{s\_\text{Target}-1} - DC = \frac{\tau_p}{\tau_s} * \frac{2\kappa_1 \cos(\omega_s \tau_1)}{\tau_{in} G_N} \tag{13}$$

where $DC' = \frac{DC + \frac{\tau_p}{\tau_s} * \left(\frac{2\kappa_2 \cos(\omega_s \tau_2)}{\tau_{in} G_N}\right)}{1 - \frac{2\tau_p \kappa_2 \cos(\omega_s \tau_2)}{\tau_{in}}}$. τ_p, τ_s and τ_{in} are LD related internal parameters, which are fixed for a certain LD. κ_2 and $\cos(\omega_s \tau_2)$ are relate to Target-2 which is stationary and located at a certain position. Therefore, DC' is constant. In the following, we call ΔP_s and $\Delta P_{s\_\text{Target}-1}$ as SMI signal with

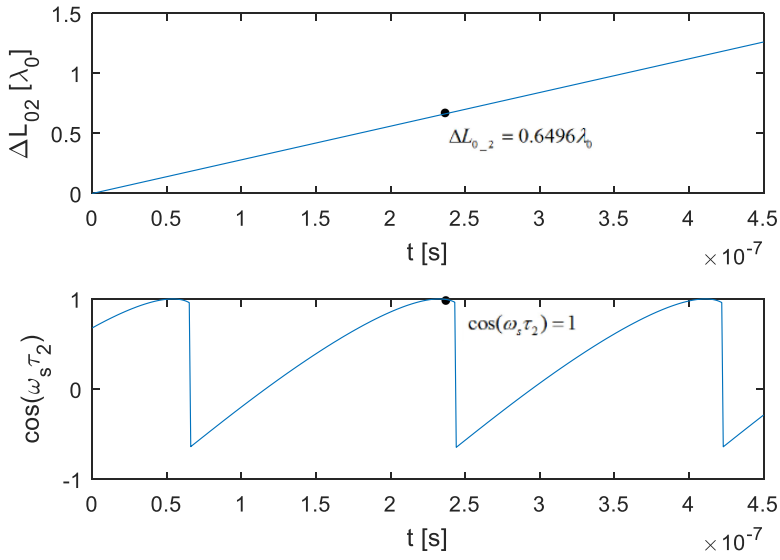

Fig. 3. Determining the location of Target-2 by $\cos(\omega_s\tau_2) = 1$ when $L_{0\_2} = 0.05$ m and $\kappa_2 = 0.0154$, (a) A varying ΔL_{0_2} and (b) Its corresponding SMI signal.

and without pe-feedback, respectively. From Eq.(12) and Eq.(13), we have,

$$\frac{\Delta P_s}{\Delta P_{s-\text{Target-1}}} = \frac{1}{1 - \frac{2\tau_p\kappa_2\cos(\omega_s\tau_2)}{\tau_{in}}} \tag{14}$$

Increasing κ_2 and setting a proper position of Target-2 to ensure that $\cos(\omega_s\tau_2) \approx 1$, we will be able to achieve $\frac{\Delta P_s}{\Delta P_{s-\text{Target-1}}} > 1$. It means that we can obtain a lager signal magnitude by using pre-feedback configuration compared to the conventional SMI with a signal target for the same displacement information.

To increase κ_2, we can employ a target with high reflectivity surface. To achieve $\cos(\omega_s\tau_2) \approx 1$, we can finely adjust its location by observing the laser intensity. The location is determined when the laser intensity reaches its highest value.

3. Simulation Verification

We implement SMI systems with both the SMI model with pre-feedback Eq.(7) and the convenitinal SMI model Eq.(8) to show how the sening sensitivity is improved. In the simulation, the LD internal parameters values are given in Table 1. The LD wavelength is $\lambda_0 = 780$ nm, and the injection current is $J = 1.1J_{th}$, where J_{th} is the injection current threshold.

To enhance the magnitude for the SMI signal with pre-feedback, firstly we need to determine the location of Target-2 (denoted by L_2). Set $L_2 = L_{0\_2} + \Delta L_{0\_2}$, where L_{0_2} is the initial cavity length. ΔL_{0_2} is a small displacement ranging from 0 to λ_0. The SMI signal in Fig. 3 is plotted by using a conventional SMI model with only Target-2 present. Fig. 3(a) shows a small varying ΔL_{0_2} applied to Target-2 and Fig. 3(b) is the corresonding SMI signal of ΔL_{0_2}. ΔL_{0_2} is determined when the SMI signal reachs its peak.

Moving Target-1 can cause a small varying ω_s. To ensure that $\cos(\omega_s\tau_2) \approx 1$, $\cos(\omega_s\tau_2)$ need to have a small variation range, which can be achieved by limts the initial length of Target-2 (L_{0_2}).

Suppose that Target-1 is at weak feedback with $\kappa_1 = 0.0002$ and the initial external cavity length $L_{0\_1} = 0.7$ m. Target-1 is in linear displacement ΔL_1. We consider two different pre-feedback strengths provided by Target-2 respectively with $\kappa_2 = 0.0154$ and $\kappa_2 = 0.0307$, the initial cavity of Target-2 is set as $L_{0\_2} = 0.05$ m.

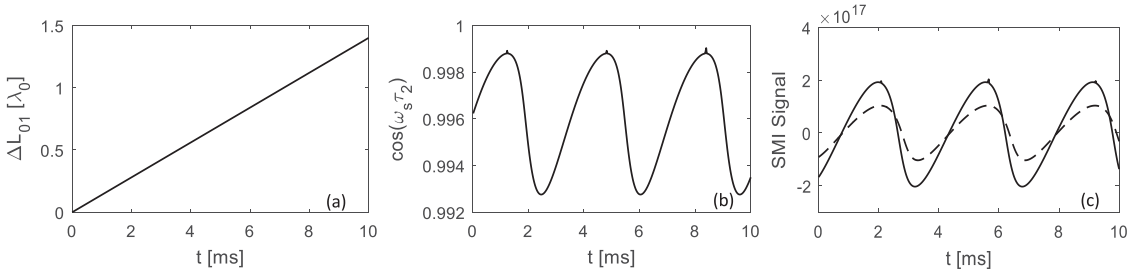

Fig. 4. Comparison of SMI signal with and without pre-feedback when $\kappa_2 = 0.0154$.

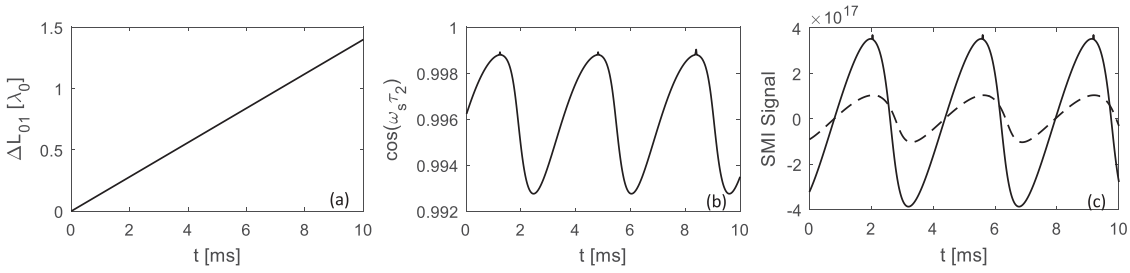

Fig. 5. Comparison of SMI signal with and without pre-feedback when $\kappa_2 = 0.0307$.

The simulation results with $\kappa_2 = 0.0154$ are shown in Fig. 4, where Fig. 4(a) is the linear displacement applied on Target-1 and Fig. 4(b) shows the variation in $\cos(\omega_s\tau_2)$ caused by Target-1. It can be seen that the location we set for Target-2 can have $\cos(\omega_s\tau_2) \approx 1$. Fig. 4(c) shows the SMI signals corresponding to the displacement in Fig. 4(a). The solid and the dashed lines respectively represent the SMI signal with and without pre-feedback. It can be seen that the magnitude of the signal with pre-feedback is enhanced by 2 times compared to the signal without pre-feedback.

Fig. 5 shows the result when the pre-feedback strength is increased to $\kappa_2 = 0.0307$ while all other parameters remain unchange. It can be seen that a larger magnitude for the SMI signal with pre-feedback is obatined, and the magnitude is enhanced by 3.7 times.

4. Experiment

To verify the proposed method, we further built an experimental system presented in Fig. 6. A single mode laser diode (Hatachi HL8325G, $\lambda_0 = 830$ nm, output power $P_0 = 40$ mW) is employed in this physical system. The LD is driven and temperature-stabilized by a LD controller (Thorlabs, ITC4001) at the injection current of 90 mA and the temperature of 23 $\pm$ 01 °C. The light emitted by the LD is focused by a lens then splited into two light beams by a beam splitter (BS) with spliting ratio of 50:50. One beam is directed to the Target-1 whose displacement is to be measured. The other beam is directed to the Target-2 for providing pre-feedback. The Target-1 is a piezoelectric transducer (PZT) (Thorlabs, PAS005). A piece of paper is glued on the PZT head to provide a weak feedback. The PZT (PAS005) has a displacement resolution of 20 nm, driven by a PZT controller (Thorlabs, MDT694) by applying a sinusoidal driving signal. Another PZT (PI P-841.20) with higher displacement resolution (9 nm) is employed as Target-2 used for providing pre-feedback. To provide a high feedback by Target-2, a mirror is glued on the head of this PZT. PZT (PI P-841.20) is driven by a controller (PI E-625). We use this PZT to finely adjust the position of Target-2 to meet the requirement of $\cos(\omega_s\tau_2) \approx 1$. A variable attenuator (VA) (Thorlabs, NDC-50C-2M-B) is inserted between the beam splitter and Target-2. The VA is continuously variable density filter with angular graduations mounted on an rotating axle which can be used to continuously adjust the pre-feedback strength, which is used to adjust the feedback strength of the pre-feedback. The photodiode (PD)

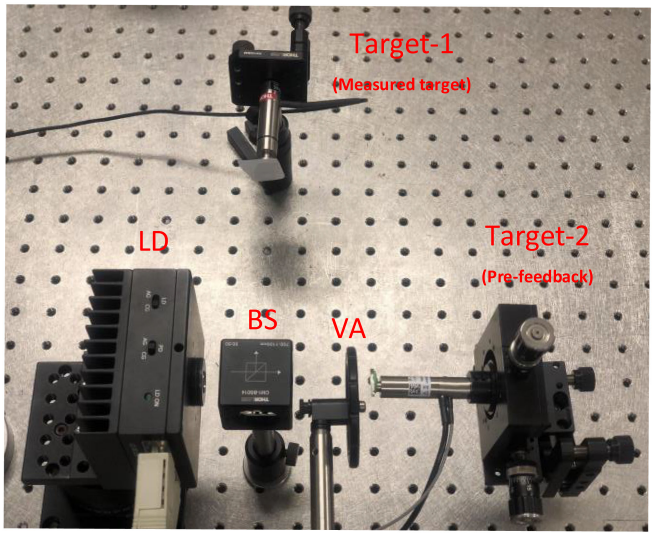

Fig. 6. SMI experimental system with pre-feedback configuration. LD: Laser Diode; BS: Beam Splitter; VA: Variable attenuator;

packaged at the rear of the LD is connected to a detection circuit to detect an SMI signal, named ΔP_s. Finally, the SMI signal is captured, recorded and displayed by a digital oscilloscope.

The experiment is carried out following the procedure as below:

1. Firstly, remove Target-2 from Fig. 6, with only Target-1, we observe an SMI signal using the experimental system established. Apply an displacement on Target-1 by PZT (PAS005). The controlling voltage signal from a signal generator applied on the PZT driver is an sinusodial signal with freqeuncy of 200 Hz,amplitude of 3 V. According to the datasheet, 0.1 V controlling voltage leads to 27 nm displacement of the PZT. The initial external cavity length of Target-1 is 0.25 m. As the surface of Target-1 has very low reflectivity, the SMI signal recorded by the oscilloscopt looks blurred, shown on Fig. 7(a).
2. Then block the light beam refected from Target-1. The system now only have optical feedback from Target-2. We adjust the location for Target-2 to meet $\cos(\omega_s \tau_2) = 1$. Rotate the VA which is located between the PZT (P-841.20) and the spiliter so that the system with Target-2 works at moderate regim. Target-2 is placed at 0.10 m away from the LD. Moving Target-2 linearly by applying a controlling valtage signal changing from 0 V to 1 V. The corresponding SMI signal can be observed and recorded by the digital oscillocope. From the signal waveform, we can lock the location of Target-2 when the signal reach its peak where we have $\cos(\omega_s \tau_2)$ close to 1. Note this PZT has a displacment resolution of 9 nm. We can use this PZT to accurately determine the location.
3. Allow the two targets on the system, the system will receive optical feedbacks from both Target-1 and Target-2. Target-1 is moving as descrined in step 1. Target-2 is stationary at the location determinded in step 2. Then, we can obtain and an SMI signal with pre-feedback, denoting it as $\Delta P_{pre\text{–}feedback}$.
4. Starting from step 3, we further finely adjust the location of Target-2 to observe the influence of its location on $\Delta P_{pre\text{–}feedback}$. The PZT (PI P-841.20) has PC controlled function. We can use a computer to adjust its movement with 10 nm each time. In this case, about 40 different positions can be set within $\lambda_0/2$. We can observe how the magnitude of $\Delta P_{pre\text{–}feedback}$ is changed with the locations.
5. At last, we observe the influence of pre-feedback strength provided by Target-2 on $\Delta P_{pre\text{–}feedback}$ by setting Target-2 at a certain location, e.g., the location obatined in step 2. Rotate the VA to get different pre-feedback strength and record the corresponding SMI signal $\Delta P_{pre\text{–}feedback}$.

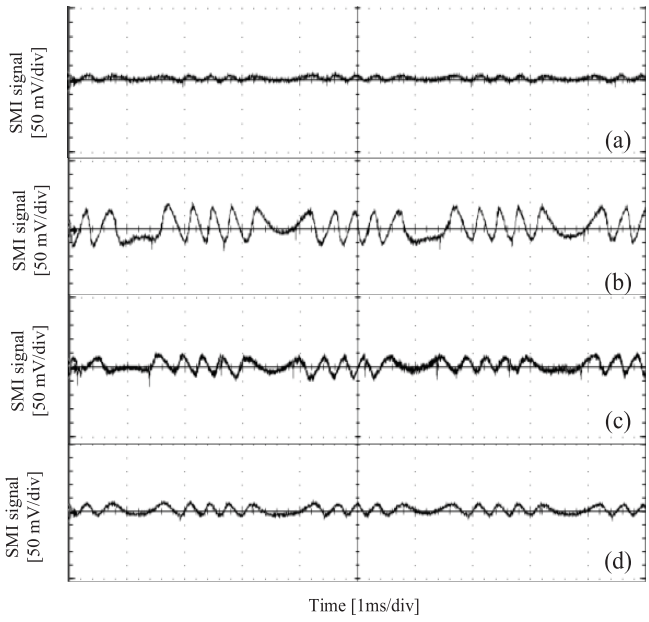

Fig. 7. Experimental results on the influence of locations of Target-2. (a) SMI signal without pre-feedback. (b), (c), (d) SMI signals with same pre-feedback strength but different position of Target-2.

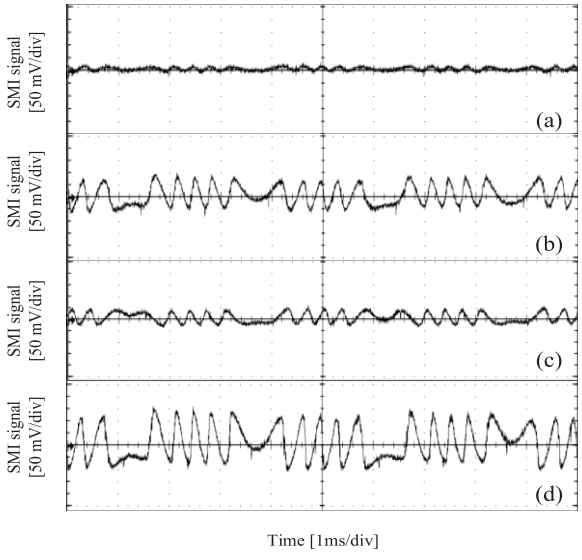

Fig. 8. Experimental results on the influence of pre-feedback strength; (a) SMI signal without pre-feedback. (b), (c), (d) SMI signals with different pre-feedback strength but same position.

The experimental results are presented in Fig. 7 and Fig. 8. Fig. 7(a) is a blurred SMI signal corresponding to the displacement of Target-1, recorded in step 1. It can be read SMI signal is nearly burried in noise. The peak-peak value of the recorded signal is about 10 mv. Note that the pre-feedback is not applied to the experimental system at this step. Fig. 7(b) is the SMI signal ($\Delta P_{pre\text{-}feedback}$) with Target-2 added to the experimental system, recorded in step 3. It shows the magnitude of the recorded signal has been significant enhanced due to the pre-feedback from Target-2. Fig. 7(c) and (d) are the SMI signals ($\Delta P_{pre\text{-}feedback}$) with same pre-feedback strength but different positions of Target-2, recorded in step 4. The peak-peak values of the SMI signals in (b),

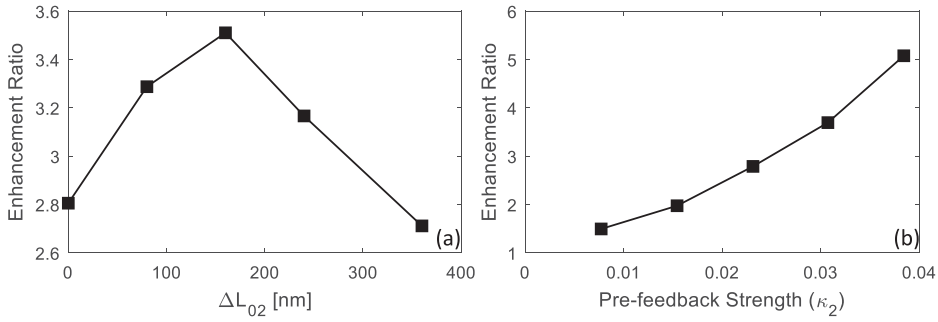

Fig. 9. Results wih different pre-feedback a) different pre-feedback cavity lengths with $\kappa_2 = 0.0327$, (b) different pre-feedback strengths with $\Delta L_{0\text{-}2} = 160$ nm.

(c) and (d) are about 35 mV, 25 mV, and 15 mV respectively. It can be seen the magnitude of SMI signal ($\Delta P_{pre\text{-}feedback}$) can be enhanced at these positions with different enhancement ratio. With the current set-up, we are able to make the blurred SMI signal more clear and enhance its magnitude to 3.5 times, shown in Fig. 7(b).

Then starting from Fig. 7(b), keeping the location of Target-2 unchanged, we change the pre-feedback strength and record the corresponding $\Delta P_{pre\text{-}feedback}$, as described in step 5. The recorded signals are shown in Fig. 8(b), (c) and (d). The signal in Fig. 8(b) is with the same position and pre-feedback strength from Target-2 as in Fig. 7(b). Fig. 8(a) is the same blurred SMI signal as in Fig. 7(a). Fig. 8(c) is the case with lower pre-feedback strength but (d) for higher strength compared to the feedback in (b). The peak-peak values in Fig. 8(b), (c) and (d) are about 20 mV, 35 mV and 50 cmV respectively, with enhancment factor as 2.0, 3.5 and 5.0. Obviously, a higher pre-feedback strength can lead to a larger magnitude in $\Delta P_{pre\text{-}feedback}$.

The more detailed influence of the location and feedback strength of Target-2 is shown in Fig. 9. Fig. 9(a) shows that the location of Target-2 needs to be choosen by satisfying $\cos(\omega_s \tau_2) = 1$ to ensure a larger ehancement ratio for a fixed pre-feedback strength. Fig. 9(b) shows that the enhancment ratio goes up with the increase of the pre-feedback strength for a fixed location of pre-feedback target. Above experiments varified the proposed SMI system with pre-feedback configuration has capability to improve the SMI signal quality in terms of large signal magnitude.

5. Conclusion

This paper proposes a new configuration for SME based displacement sensor. In this configuration, an LD has dual external cavities. One is for providing a pre-feedback and the other for the target to be measured. Both theory and experiment indicate that the pre-feedback cavity enable the overall sensing system to achieve high sensitivity for the case when the target to be measured has a very low reflectivity. The pre-feedback cavity should be chosen with a high reflectivity surface and its location can be determined by observing the sensing signal from the SME system with only the pre-feedback cavity. The presented in this paper provides important guidance for designing a practical SME based displacement sensor.

References

[1] S. Donati, G. Giuliani, and S. Merlo, "Laser diode feedback interferometer for measurement of displacements without ambiguity," *IEEE J. Quantum Electron.*, vol. 31, no. 1, pp. 113–119, Jan. 1995.
[2] Y. Yu, J. Xi, and J. F. Chicharo, "Measuring the feedback parameter of a semiconductor laser with external optical feedback," *Opt. Exp.*, vol. 19, no. 10, pp. 9582–9593, May 9, 2011.
[3] S. Donati, "Developing self-mixing interferometry for instrumentation and measurements," *Laser Photon. Rev.*, vol. 6, no. 3, pp. 393–417, 2012.
[4] L. Scalise and N. Paone, "Laser Doppler vibrometry based on self-mixing effect," *Opt. Lasers Eng.*, vol. 38, no. 3, pp. 173–184, Sep. 1, 2002.

[5] M. Wang, M. Lu, H. Hao, and J. Zhou, "Statistics of the self-mixing speckle interference in a laser diode and its application to the measurement of flow velocity," *Opt. Commun.*, vol. 260, no. 1, pp. 242–247, Apr. 1, 2006.
[6] D. Guo, H. Jiang, L. Shi, and M. Wang, "Laser self-mixing grating interferometer for MEMS accelerometer testing," *IEEE Photon. J.*, vol. 10, no. 1, Feb. 2018, Art. no. 6800609.
[7] U. Zabit, T. Bosch, and F. Bony, "Adaptive transition detection algorithm for a self-mixing displacement sensor," *IEEE Sensors J.*, vol. 9, no. 12, pp. 1879–1886, Dec. 2009.
[8] U. Zabit, F. Bony, T. Bosch, and A. D. Rakic, "A self-mixing displacement sensor with fringe-loss compensation for harmonic vibrations," *IEEE Photon. Technol. Lett.*, vol. 22, no. 6, pp. 410–412, Mar. 2010.
[9] M. T. Fathi and S. Donati, "Thickness measurement of transparent plates by a self-mixing interferometer," *Opt. Lett.*, vol. 35, no. 11, pp. 1844–1846, Jun. 1, 2010.
[10] Y. Fan, Y. Yu, J. Xi, and J. F. Chicharo, "Improving the measurement performance for a self-mixing interferometry-based displacement sensing system," *Appl. Opt.*, vol. 50, no. 26, pp. 5064–5072, Sep. 10, 2011.
[11] T. Taimre *et al.*, "Laser feedback interferometry: A tutorial on the self-mixing effect for coherent sensing," *Adv. Opt. Photon.*, vol. 7, no. 3, pp. 570–631, Sep. 30, 2015.
[12] S. Zhang, S. Zhang, Y. Tan, and L. Sun, "A microchip laser source with stable intensity and frequency used for self-mixing interferometry," *Rev. Sci. Instrum.*, vol. 87, no. 5, 2016, Art. no. 053114.
[13] M. Norgia, D. Melchionni, and A. Pesatori, "Self-mixing instrument for simultaneous distance and speed measurement," *Opt. Lasers Eng.*, vol. 99, pp. 31–38, 2017.
[14] K. Lin *et al.*, "A fiber-coupled self-mixing laser diode for the measurement of young's modulus," *Sensors (Basel, Switzerland)*, vol. 16, no. 6, 2016, Art. no. 928.
[15] J. Perchoux *et al.*, "Current developments on optical feedback interferometry as an all-optical sensor for biomedical applications," *Sensors (Basel, Switzerland)*, vol. 16, no. 5, 2016, Art. no. 694.
[16] B. Liu *et al.*, "Laser self-mixing fiber Bragg grating sensor for acoustic emission measurement," *Sensors*, vol. 18, no. 6, 2018, Art. no. 1956.
[17] R. Lang and K. Kobayashi, "External optical feedback effects on semiconductor injection laser properties," *IEEE J. Quantum Electron.*, vol. 16, no. 3, pp. 347–355, Mar. 1980.